TEXT TRAIL:
A Robust Text Tracking Algorithm In Wild Environments

Myriam Robert-Seidowsky[1], Jonathan Fabrizio[1] and Séverine Dubuisson[2]

[1] *LRDE-EPITA, 14-16, rue Voltaire, F-94276, Le Kremlin Bicêtre, France*

[2] *CNRS, UMR 7222, ISIR, F-75005, Paris, France*

myriam, jonathan@lrde.epita.fr, severine.dubuisson@isir.upmc.fr

Abstract: In this paper, we propose *TextTrail*, a new robust algorithm dedicated to text tracking in uncontrolled environments (strong motion of camera and objects, partial occlusions, blur, *etc.*). It is based on a particle filter framework whose correction step has been improved. First, we compare some likelihood functions and introduce a new one which integrates tangent distance. We show that this likelihood has a strong influence on the text tracking performances. Secondly, we compare our tracker with a similar one and finally an example of application is presented. *TextTrail* has been tested on real video sequences and has proven its efficiency. In particular, it can track texts in complex situations starting from only one detection step without needing another one to reinitialize the model.

1 INTRODUCTION

With the increasing amount of videos, automatic text extraction has become an essential topic in the computer vision application field. Whereas many works have already been published on text detection and its extraction in single images, video context has been still little investigated. To extend detection process from an image to a video sequence, a simple way is to apply a detector on each frame. However, this is not optimal. First, because the detection process may be very time consuming, especially for high textured frames. Secondly, because this "naive" approach does not provide the matching information between detections in consecutive frames. However, these associations are needed for some applications. Visual tracking algorithms are a solution for such purpose: they attempt to predict the position of text areas at each time step by using previous information and then provide some stability of detections or estimations with time. We could cite a lot of target applications for which text tracking is important, such as automatic text extraction for indexation, text-to-speech (for example for visually-impaired persons) or online text translation (for example for tourists). In these cases, tracking can improve the final transcription through redundant information and provides only one transcription per text area. It can also be fundamental in online text removal: if one specifies a text to erase within a frame, a removal process can be automatically propagated over the whole sequence by using inpainting algorithms. Thus, the main goal of text tracking is to collect a list of associated text regions throughout a sequence by minimizing the number of detection steps, as this step can be very time consuming.

State of the art about text tracking is quite restricted. Phan *et al.* (Phan et al., 2013) used the Stroke Width Transform to estimate a text mask in each frame. SIFT descriptors in keypoints from the mask are extracted and matched between two frames. Because only text pixels are tracked, it is robust to background changes but, unfortunately, only handles static or linear motions. Most of recent approaches (Tanaka and Goto, 2008; Merino and Mirmehdi, 2007; Minetto et al., 2011) use a particle filter. Merino *et al.* (Merino and Mirmehdi, 2007) proposed a method for text detection and tracking of outdoor shop signs or indoor notices, that handles both translations and rotations. Here, SIFT descriptors are computed in each component of a detected word (that is supposed to be a letter). Tanaka *et al.* (Tanaka and Goto, 2008) suggested two schemes for signboard tracking: (i) a region-based matching using RGB colors, and (ii) a block-based matching. In all prior algorithms, also known as *tracking-by-detection*, text is first detected in each frame, then "tracked" between frames, by using a matching step that associates detected text areas. However, a recent

algorithm, *Snoopertrack* (Minetto et al., 2011), detects text every 20 frames, and tracks it between them, using HOGs as feature descriptors.

In this paper, we focus on text tracking. Our algorithm, called *TextTrail* relies on the particle filter framework, well known to handle potential erratic and fast motion. Our tracker is initialized using our previous work on text localization in single images (Fabrizio et al., 2013). This detector is restricted to block letters text in a Latin alphabet, but could easily be extended to other alphabet by adapting its learning process. Compared to the state of the art, our algorithm *TextTrail* can accurately track text regions during a long time (hundreds of frames) without needing to reinitialize the model(s) with new detections. We introduce a new likelihood used in the correction step of the particle filter which uses the tangent distance between grayscale patches. This likelihood function has been studied and compared with other ones including common ones relying on Bhattacharyya distance between HOG descriptors (Medeiros et al., 2010; Tuong et al., 2011; Breitenstein et al., 2009). Our tests show that the tangent distance is really suitable for text tracking purposes. The paper is organized as follows. In Section 2 we quickly introduces the particle filter and the tangent distance. Then, in Section 3, we expose different likelihoods for text tracking before proposing a new one (the one we use in *TextTrail*). We compare them in Section 4 and evaluate *TextTrail* performances. We also compare our approach with a similar one. In addition we illustrate its interest by integrating it into a complete scheme of application. Concluding remarks are finally given in Section 5.

2 BACKGROUND

2.1 Particle Filter

The particle filter (PF) framework (Gordon et al., 1993) aims at estimating a state sequence $\{\mathbf{x}_t\}_{t=1,\ldots,T}$, whose evolution is given, from a set of observations $\{\mathbf{y}_t\}_{t=1,\ldots,T}$. From a probabilistic point of view, it amounts to estimate for any t, $p(\mathbf{x}_t|\mathbf{y}_{1:t})$. This can be computed by iteratively using Eq. (1) and (2), which are respectively referred to as a prediction step and a correction step.

$$p(\mathbf{x}_t|\mathbf{y}_{1:t-1}) = \int_{\mathbf{x}_{t-1}} p(\mathbf{x}_t|\mathbf{x}_{t-1})p(\mathbf{x}_{t-1}|\mathbf{y}_{1:t-1})d\mathbf{x}_{t-1} \quad (1)$$

$$p(\mathbf{x}_t|\mathbf{y}_{1:t}) \propto p(\mathbf{y}_t|\mathbf{x}_t)p(\mathbf{x}_t|\mathbf{y}_{1:t-1}) \quad (2)$$

In this case, $p(\mathbf{x}_t|\mathbf{x}_{t-1})$ is the transition and $p(\mathbf{y}_t|\mathbf{x}_t)$ the likelihood. PF aims at approximating the above

distributions using weighted samples $\{\mathbf{x}_t^{(i)}, w_t^{(i)}\}$ of N possible realizations of the state $\mathbf{x}_t^{(i)}$ called *particles*. In its basic scheme, PF first propagates the particle set $\{\mathbf{x}_{t-1}^{(i)}, w_{t-1}^{(i)}\}$ (Eq. (1)), then corrects particles' weights using the likelihood, so that $w_t^{(i)} \propto p(\mathbf{y}_t|\mathbf{x}_t^{(i)})$, with $\sum_{i=1}^N w_t^{(i)} = 1$ (Eq. (2)). The estimation of the posterior density $p(\mathbf{x}_t|\mathbf{y}_{1:t})$ is given by $\sum_{i=1}^N w_t^{(i)} \delta_{\mathbf{x}_t^{(i)}}(\mathbf{x}_t)$, where $\delta_{\mathbf{x}_t^{(i)}}$ are Dirac masses centered on particles $\mathbf{x}_t^{(i)}$. A resampling step can also be performed if necessary.

2.2 Tangent Distance

Tangent Distance (TD) allows to robustly compare two patterns against small transformations. It was first introduced by Simard *et al.* (Simard et al., 1992) and was mostly used for character recognition (Schwenk and Milgram, 1996), but also for face detection and recognition (Mariani, 2002), speech recognition (Macherey et al., 2001) and motion compensation (Fabrizio et al., 2012).

To compare two patterns *I* and *J*, the Euclidean distance is not efficient as these two patterns may undergo transformations. With TD, a set of potential transformations is modeled. As these transformations are not linear, we consider an approximation with linear surfaces. Here, the Euclidean distance is not computed between the two patterns, but between the two linear surfaces. Obviously, amplitudes of these transformations are unknown. In our case, we model transformations only on one pattern (in this example *J*). If we note $d_{\mathrm{ec}}(.,.)$ the Euclidean distance, the TD is:

$$min(d_{\mathrm{ec}}(I, J + \sum_{i=1}^M \lambda_i V_i)) \quad (3)$$

with V_i the tangent vector of *i*-th modeled transformation and λ_i its contribution. In this minimization scheme, *I* and *J* are known. Tangent vectors can be computed numerically or analytically. On the contrary, all coefficients λ_i are unknown: the result of the minimization gives their optimal values.

3 PROPOSED APPROACH

3.1 Framework

We propose an algorithm which robustly tracks multiple text areas in video sequences using a PF. For the initialization step, text regions are detected in the first frame using the detector proposed in (Fabrizio et al., 2013), and used as models in the rest of the sequence

without any update. We use one PF per model to track. Note that we initialize once our tracker in order to see how long the algorithm can track text areas without needing updating their models: we can then not detect text that appears over time. The dimension of the box surrounding each text area is supposed to be constant: the state vector $\mathbf{x}_t$ of each PF contains the coordinates (x, y) of its top left corner. Because no prior knowledge on motion is taken into account, particles are propagated within a very large search space (circle of radius 40 pixels). Each particle $\mathbf{x}_t^{(i)}$, $i = 1, \ldots, N$ (with $N = 200$) is here an hypothetical state (*i.e.* a possible position for the tracked text area top left corner). Its weight is given by $w_t^{(i)} = e^{-\alpha d^2}$, with d a distance between the description of the particle and the one of the model, and the correction parameter α a positive value to fix (see Section 4). When the region of a particle is partially outside the image, its description is computed only into its visible part and ditto for the model. Note that, at each iteration of a PF, a basic multinomial resampling is performed from the discrete distribution given by the normalized weights $w_t^{(i)}$.

One of the main challenges in tracking algorithms is to ascertain which feature descriptors and distance d between them best discriminate the tracked object from the rest of the frame. The particles' weights should be the most relevant possible. Below, we compare two distances (Bhattacharyya distance (Bhattacharyya, 1943) and TD previously exposed) integrating different descriptors.

3.2 Bhattacharyya Distance between HOGs and extension

As feature descriptors for text area(s) to track, an HOG (Dalal and Triggs, 2005) is computed into each text area by quantizing gradient orientations into 9 bins (8 orientations plus an extra bin for counting the negligible gradient amplitudes *i.e.* homogeneous zones). A particle and the model can be compared by computing the Bhattacharyya distance (BD) noted d_{bd} between their corresponding normalized HOG.

If we consider two normalized histograms P and Q with p_i (resp. q_i) the ith bins of P (resp. Q), $i = 1, \ldots, B$ with B the number of bins in the histograms, the BD between P and Q is given by:

$$d_{bd} = \sqrt{1 - \sum_{i=1}^{B} \sqrt{P(p_i)Q(q_i)}} \qquad (4)$$

The particles' weights are given by $w_t^{(i)} = e^{-\alpha d_{bd}^2}$. One of the drawback of HOG is that it does not integrate spatial information, and then not the shape of

letters. To overcome this limitation, we extend HOG to Revisited Histogram of Oriented Gradient (RHOG) by:

1. Computing HOG in the mask provided by the segmented letters of the model given by the algorithm in (Fabrizio et al., 2013) (Fig. 1) ;

2. Dividing the text area into 3×3 blocks and computing HOG in each block.

BDs are separately computed (on the 9 blocks and on segmented letters) then averaged. If computing BD between RHOGs permits to refine the likelihood function, it can however not handle rotations or scale changes for example. That is why, to be robust to small transformations, we introduce the TD into the PF.

(a) Examples of particles with the mask used to restrict the computation of HOG (b)
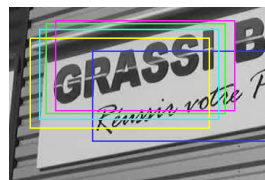
(b) Position of particles and model in the current frame

(c) The model with the deduced mask

Figure 1: For each particle (a), HOG is computed into the area restricted to the mask provided by the segmented letters of the model (c).

3.3 Tangent Distance Between Gray Level Patches

Let J be the text area model and I the particle area (both corresponding to gray level image patches). We here consider $M = 3$ possible transformations of J: horizontal and vertical stretching and rotation. First, tangent vectors V_i, $i = 1, \ldots, M$ are computed from each model text areas only once in the algorithm. Then, by minimizing the difference between I and J (Section 2.2), we get contributions λ_i for each transformation. Applying these coefficients λ_i to the model provides a prediction area noted K. Finally, the TD noted d_{td} is the difference pixel per pixel between prediction K and particle I. The particles' weights are then computed so that $w_t^{(i)} = e^{-\alpha d_{td}^2}$. The usage of TD allows the tracker to handle small rotations and small

scale changes. We could have considered other transformations such as illumination changes for example but it would have been more time consuming.

3.4 BD and TD Combination

To compare the two previous distances *i.e.* BD and TD, we have generated 3D surfaces defined as follows. A text model was extracted in the first frame of a sequence (magenta rectangle and contours of segmented letters, Fig. 2.(a)). The search space is defined in frame 6 as the square of 40×40 pixels centered on the previous top left corner estimation of the tracked text area (red square, Fig. 2.(b)). We have chosen this example because some text areas are visually similar to the model in this search space (the text *epicerie* to track had similar color and shape to *kebbab*, *pizza* and *boissons*). The distances are computed in each pixel of this search space, giving surfaces shown in Fig. 2.(c-e). These distance surfaces should have a global minimum around the solution (close to the top left corner location of the tracked text area) and a slope to reach it. In such cases, $w_t^{(i)} = e^{-\alpha d^2}$ should have high values.

Fig. 2.(c) shows the surface given by BD between RHOGs: (BD(RHOG)). We can see that further particles have a high distance but this surface has no peaked global minimum but rather presents a valley along the text direction (horizontal). Then, all particles located in this latter have a high weight, even if they are far from the solution. PF will provide an estimation in any point along the bottom of this valley. That is not satisfactory because too much imprecise.

Fig. 2.(d) shows the surface given by TD between gray level patches. It presents good properties to precisely localize the solution into a global minimum. Unfortunately, the region around this global minimum is too peaked. As this region is too narrow, only few particles with high weight will contribute to the estimation (weighted sum) of the tracked text. Elsewhere TD gives approximately the same high values which means that particles' weights are low and irrelevant. As (BD(RHOG)), TD seems not to be reliable because, integrated into PF, it requires that at least a few particles are drawn near the solution. If not, PF will diverge and then fail.

To take advantage of both presented configurations, we propose to combine (multiply) BD(RHOG) and TD. The usage of this combination (noted BD(RHOG)×TD) in a particle filter gives a robust text tracker. It is our selected solution called *TextTrail*. The result of the combination is shown in Fig. 2.(e). This surface has both the property of BD(RHOG) to converge to the solution (valley), and the precision of its localization (peak of TD surface). Thus, particles' weights will be computed so that $w_t^{(i)} = e^{-\alpha(d_{bd} \times d_{td})^2}$.

4 EXPERIMENTAL RESULTS

In this section, we evaluate *TextTrail*, our text tracking algorithm. First, we compare several likelihood functions used in the framework of the PF: common ones and new ones we build. We especially focus on the impact of the TD on tracking performances to validate the likelihood function we have introduced. We have created a batch of video to prove the robustness of our method. Secondly, we intended to compare *TextTrail* with other algorithms but unfortunately only a few are dedicated to text tracking and none provides source codes. Nevertheless, performances of *Snoopertrack* (Minetto et al., 2011) are given, and datasets are online available, so we can compare our method with their. Finally, to illustrate an interest of our method, we integrate our text tracker into a complete framework dedicated to online text removing in video sequences.

4.1 Likelihood Evaluation

4.1.1 Our challenging dataset

To test the robustness of several likelihood functions, the dataset must be as challenging as possible. Our dataset contains seven 1280×720 pixel video sequences, captured in wild environment *i.e.* under unconstrained conditions in natural scenes (indoor and outdoor environments). These video and their associated ground truth (GT) are in the same XML format as in ICDAR (ICDAR, 2013) and publicly available[1]. Note that texts in those video are affected by many and varied difficulties such as: translations, rotations, noise, stretching, changing in point of view, partial occlusions, cluttered backgrounds, motion blur, low contrast, *etc.* Moreover, same texts can be close to each others and share visual similarities, thus perturb trackers. Fig. 4 shows some frame examples for each video used in our experiment part.

4.1.2 Comparison of configurations

We compare the efficiency of 5 trackers relying on different configurations: BD(HOG), BD(RHOG), TD, BD(HOG)×TD and BD(RHOG)×TD). For all of them, the model(s) is(are) initialized in the first frame from their corresponding GT, then tracked

---

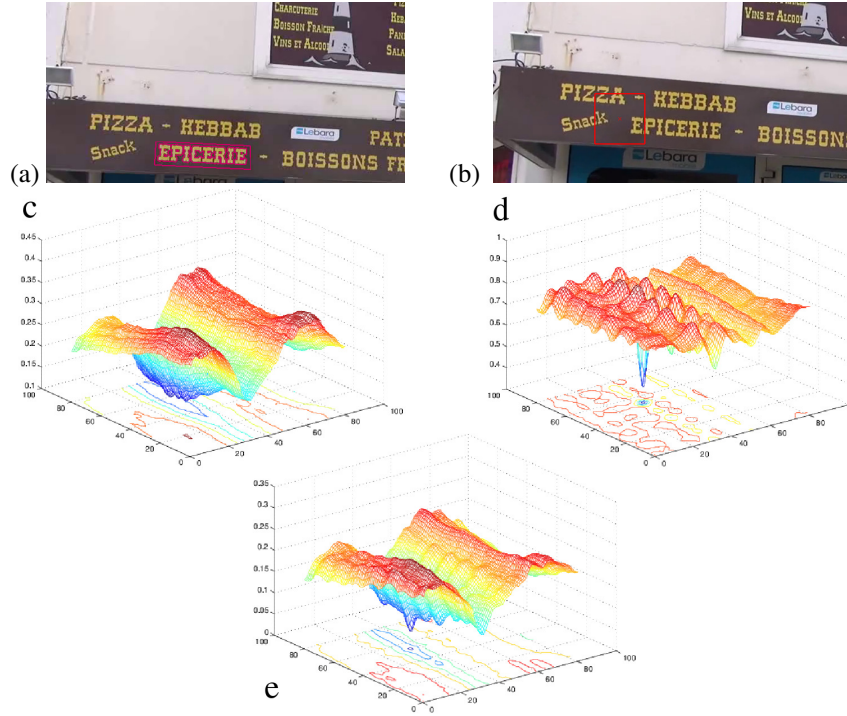[1] https://www.lrde.epita.fr/~myriam

Figure 2: Distance surfaces (c-e) computed between each area and the model ((a) magenta) in each pixel of the search space ((b) red). Surfaces are obtained with (c) BD(RHOG), (d) TD and, (c) combination of BD(RHOG) and TD.

during 100 to 200 frames without any update of model(s). To evaluate and compare the different configurations, we compute the *Fscore* which combines precision and recall, given by:

$$Precision = \frac{Overlap}{Surface_{Track}} \qquad Recall = \frac{Overlap}{Surface_{GT}}$$

$$Fscore = \frac{2 \times (Precision \times Recall)}{Precision + Recall}$$

This measure depends on the spatial overlap between the non-rectangular areas of GT and prediction from the tracker. $Surface_{Track}$ is the number of pixels in the predicted region and $Surface_{GT}$ is the number of pixels in the GT. *Overlap* is the number of pixels in both previous surfaces. Note that, because no one of our proposed configurations handles size change while GT does, it is impossible to reach a *Fscore* of 100% even if, visually the tracking seems to be correct. Due to the stochastic nature of PF, each tracker's *Fscore* is an average over 50 runs. Note that the correction parameter α used for weight computation has a strong influence on the performance of the tracker: it reshapes the profile of the likelihood (Lichtenauer et al., 2004) (Fontmarty et al., 2009) (Brasnett and Mihaylova, 2007). Therefore, for a fair comparison between each configuration, we tuned its α so that it yields best tracking results.
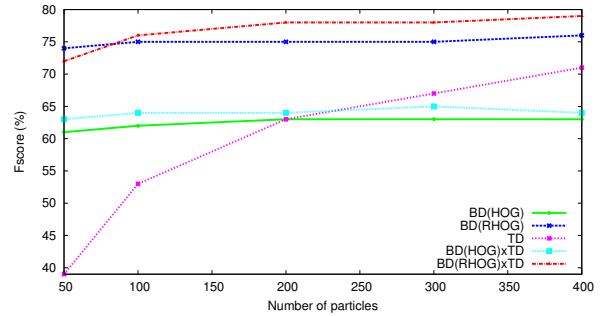

Figure 3: Convergence curves.

4.1.3 Likelihood selection

Fig. 3 shows evolutions of *Fscore* values (average over 50 runs for each tracked text areas in all test sequences) when number of particles N increases. One can note that TD needs a lot of particles to achieve a high *Fscore*. BD(HOG), BD(RHOG) and BD(HOG)×TD are more stable since they quickly converge. Best *Fscore*s are provided by BD(RHOG)×TD (red curve) from $N = 100$ and are still slowly increasing with N. As most *Fscore*s are stabilized from $N = 200$, we have chosen to perform our tests with this number of particles.

Table 1 presents *Fscore*s (average over 50 runs for each tracked text areas in all test sequences) with $N = 200$. For each *Fscore*, the standard deviation over the 50 runs is given in square bracket.

We can observe that TD often gives best *Fscore* results, combined with BD(RHOG) or not. Because of the too much peaked global minimum of TD (see Section 3), its results are not stable: *Fscore*s can be either high (*Laverie*) or low (*Voyage*). Its standard deviation is higher than other ones. Therefore, the unreliability of TD makes it unusable alone. When it low-performs, its combination with BD(RHOG) allows to reach an higher *Fscore* (see for example the case of words *Fumer* or *Voyage*).

Notice also, that the RHOG always improves results compared to HOG (except for *Service*) when it is used alone or combined with the TD. This confirms that the addition of the computation of the HOG on the boundaries of letters is a powerful improvement.

On words *Service*, all results are poor. In fact, the two occurrences of word *Service* (Fig. 4.1) affect all trackers because these words are swapped while tracking. This explains also the high standard deviation of trackers.

Over all tracked texts, our text tracker (called *Text-Trail*) with BD(RHOG)×TD combination, gives on average the higher *Fscore* (78.3%) on our challenging video sequences. These experiments have shown that it is efficient and outperforms a classical approach like BD(HOG). It takes advantages of both approaches, the global coarse solution of the BD(RHOG) and the local and precise solution of the TD.

4.2 Comparison with another approach

Here, we compare our *TextTrail* with *Snooper-Track* (Minetto et al., 2011) in terms of scores and computation times. Algorithm *SnooperTrack* relies on detection steps processed every 20 frames: model(s) of their tracked text(s) are then regularly updated. On the contrary, our method only initializes models by detecting text areas in the first frame and keeps the corresponding model(s) constant during the whole sequence. These approaches are not "fairly comparable" but *SnooperTrack* seems to be the most similar online available algorithm. The comparison is done on their dataset which is publicly available using evaluation protocol described in (Lucas, 2005). Note that our algorithm has been executed on a machine Intel i5-3450$^{©}$, 3.1GHz, 8GB of RAM, coded in C++ with our library Olena (Levillain et al., 2010) without optimization.

Table 2 gives for each video of the dataset, recalls, precisions, *Fscore*s and average processing times per frame obtained by *TextTrail* and *SnooperTrack*.

One can see that in average on these 5 sequences, *TextTrail* reaches the higher *Fscore* (0.67) and the higher precision (0.74) rates. Moreover, it is on average more than two times faster (0.21 sec. per frame) than the other method (0.44 sec. per frame). Note that we do not know if computation times of *SnooperTrack* also include detection times or just tracking. Apart for the video "Cambronne", our average computation times are 5.5 times faster (0.0775 sec. per frame). Note that "Cambronne" sequence is particular as it contains many text areas localized on the frame borders: models, restricted to the visible part of the particle, have to be recomputed. We have not optimized this part of our algorithm, which explains the higher computation times obtained for this video.

Our precision rates are always higher (0.74 vs. 0.61). This shows our prediction areas most of times is included in the GT. However, our recall rate is lower (0.62 vs. 0.69). As our model size is fixed over time, even if TD handle small size changes, our predicted text area size does not change. This is why our recall rates are smaller. Our predictions of text areas are then well localized but the scale is not well adapted to the GT to get higher recall rates.

Furthermore, "v04-Navette" sequence shows an explicit example of limitation of our approach. In this video, text area sizes are hardly changing with time. Our algorithm succeeds to track text up the TD reaches its limits *i.e.* when it can not manage high scale changes. This is why we added a simple criterion (based on the difference of prediction scores in successive frames *i.e.* weight(s) of predicted text area(s)) to stop our tracker(s) in such cases.

Thanks to the TD, robust to small transformations, this is not necessary to include the corresponding transformation parameters (scale, for example) into the state. The state space dimension is then reduced and we need fewer particles to get an efficient tracking.

Without updating the model, *TextTrail* can track during hundreds of frames, that prove its robustness. In practice, to manage apparitions or high changes in the model (occlusions, illumination, *etc.*), a detection step can be launched more often. But, compared to *SnooperTrack*, we can track during more than 20 frames without needing to restart tracking from new detections.

4.3 Application: text removal

This section is dedicated to an example of application of our text tracker. Our goal is to remove text superimposed on frames of a video sequence. *Text-*

Figure 4: Our challenging video sequences. 1-2: motion blur, 3-4: partial occlusion, 5: rotation, 6: cluttered background. Zoom on text models to track (extracting from the first frame) are given above each frame.

Tracked texts	BD(HOG)		BD(RHOG)		TD		BD(HOG)×TD		BD(RHOG)×TD		# Frames
Fig.3.1. LAVERIE	76.49	[0.60]	89.98	[1.70]	**96.45**	[0.36]	77.51	[1.02]	95.00	[0.84]	71
Fig.3.1. LIBRE	59.64	[1.88]	77.12	[1.06]	79.02	[7.71]	67.77	[7.08]	**84.16**	[7.61]	71
Fig.3.1. SERVICE	46.42	[2.34]	46.02	[10.29]	**52.34**	[13.27]	46.24	[2.65]	47.90	[9.2]	71
Fig.3.1. WASH	58.85	[1.22]	64.61	[1.36]	73.08	[8.14]	64.92	[2.84]	**74.50**	[3.90]	71
Fig.3.1. SERVICE	31,31	[2.07]	44,93	[7.88]	**53,44**	[4.81]	32,88	[1.79]	51,74	[10.59]	71
Fig.3.2. DEFENSE	82.69	[0.90]	86.35	[1.39]	72.73	[12.29]	82.73	[0.91]	**87,55**	[4.75]	207
Fig.3.2. FUMER	37.61	[8.46]	78.24	[4.68]	48.51	[28.09]	53.97	[5.21]	**84.61**	[6.71]	207
Fig.3.3. THERMOS	58.10	[2.76]	78.29	[0.11]	**87.59**	[0.04]	62.04	[4.57]	78.15	[0.34]	134
Fig.3.4. RESTAURANT	83.40	[0.62]	**88.93**	[0.20]	47.46	[3.98]	61.10	[15.46]	81.75	[0.54]	201
Fig.3.5. CONTROL	75.83	[0.25]	78.76	[0.40]	83.32	[0.19]	78.11	[0.44]	**83.47**	[0.11]	131
Fig.3.6. VOYAGE	86.50	[0.81]	**95.34**	[1.38]	9.37	[7.97]	84.04	[0.56]	92.44	[1.50]	159
Mean	63.35		75.32		63.94		64.66		**78.30**		
Std	19.18		16.90		24.72		15.94		**15.24**		

Table 1: *Fscore*s for all trackers with their optimal α value and $N = 200$. Max *Fscores* per text are represented in bold and max average *Fscores* and min standard deviations in red.

Trail can locate the text to remove in each frame. This text is then removed using a classical inpainting algorithm (Bertalmio et al., 2001). In practice, we manually select a text area in the first frame of the video sequence, which is automatically tracked during the sequence. A binarization process then provides a mask which precisely cutouts the text letters. The inpainting is automatically processed in each frame using this mask.

Fig. 5 presents different frames of a video from our dataset: frames with superimposed texts, after the tracking and binarization process and finally results of the inpainting procedure. One can see that the text is correctly localized and then removed. Even if the result is not "visually perfect", no one can identify that something was erased.

5 CONCLUSIONS

In this article, we have presented *TextTrail*, a new algorithm for multiple text tracking in complex video sequences relying on a particle filter framework. Even if the particle filter framework is well known, the novel idea here, is to combine the Bhattacharyya and tangent distances in order to increase the efficiency of the correction step which leads to a more robust text tracker. According to our experiments, tangent distance on gray level patches gives a good precision of the text and Bhattacharyya distance between "revisited" HOGs adds information on the shape of letters. High likelihood areas are well localized and sufficiently smooth for the particle filter to keep a diversity of its state representation (*i.e.* position of the tracked text area) *via* the particle set. Unlike classical approaches from the literature, we show that our method can track text areas during long times in video sequences containing complex situations (motion blur, partial occlusion, *etc.*) starting from only one detection step, that is less time consuming. Indeed, our tracker is initialized by a detection step and models are never updated, proving the efficiency of the method. We also show our tracking can be embedded into a complete framework dedicated to text removal. If future works, we plan to overcome the limitation of our approach and allow to manage stronger transformations. A simple solution is to add frequent detections to update the model(s). Another solution is to extend the state space (add scale parameters for example). Usually, increasing the state space means increasing the number of particles to achieve good tracking performances. But, because tangent distance can also handle small transformations, state space should be sampled more coarsely, then using fewer particles. We think that, even if we increase the state space dimension, we probably will need fewer particles to achieve lower tracking errors, and then also reduce the computation times.

REFERENCES

Bertalmio, M., Bertozzi, A. L., and Sapiro, G. (2001). Navier-stokes, fluid dynamics, and image and video inpainting. In *CVPR*, pages 355–362.

Bhattacharyya, A. (1943). On a measure of divergence between two statistical populations defined by their probability distributions. *Bulletin of Cal. Math. Soc.*, 35(1):99–109.

Brasnett, P. and Mihaylova, L. (2007). Sequential monte carlo tracking by fusing multiple cues in video sequences. *Image and Vision Computing*, 25(8):1217–1227.

Breitenstein, M. D., Reichlin, F., Leibe, B., Koller-Meier, E., and Gool, L. V. (2009). Robust tracking-by-detection using a detector confidence particle filter. In *ICCV*, pages 1515–1522.

Dalal, N. and Triggs, B. (2005). Histograms of oriented gradients for human detection. In *CVPR*, pages 886–893.

Fabrizio, J., Dubuisson, S., and Béréziat, D. (2012). Motion compensation based on tangent distance prediction for video compression. *Signal Processing: Image Communication*, 27(2):153–171.

Fabrizio, J., Marcotegui, B., and M.Cord (2013). Text detection in street level image. *Pattern Analysis and Applications*, 16(4):519–533.

Fontmarty, M., Lerasle, F., and Danes, P. (2009). Likelihood tuning for particle filter in visual tracking. In *ICIP*, pages 4101–4104.

Gordon, N., Salmond, D., and Smith, A. (1993). Novel approach to nonlinear/non-Gaussian Bayesian state estimation. *IEE Proc. of Radar and Signal Processing*, 140(2):107–113.

ICDAR (2013). ICDAR 2013 robust reading competition, challenge 3: text localization in video. http://dag.cvc.uab.es/icdar2013competition/?ch=3.

Levillain, R., Geraud, T., and Najman, L. (2010). Why and howto design a generic and efficient image processing framework: The case of the milena library. In *ICIP*, pages 1941–1944.

Lichtenauer, J., Reinders, M., and Hendriks, E. (2004). Influence of the observation likelihood function on object tracking performance in particle filtering. In *FG*, pages 227–233.

Lucas, S. M. (2005). Text locating competition results. In *Proceedings of the Eighth International Conference on Document Analysis and Recognition*, ICDAR '05, pages 80–85.

Macherey, W., Keysers, D., Dahmen, J., and Ney, H. (2001). Improving automatic speech recognition using tangent distance. In *ECSCT*, volume III, pages 1825–1828.

Video	Recall		Precision		*Fscore*		T(s)	
	SnooperTrack	*TextTrail*	*SnooperTrack*	*TextTrail*	*SnooperTrack*	*TextTrail*	*SnooperTrack*	*TextTrail*
v01-Bateau	**0.80**	**0.80**	0.55	**0.80**	0.63	**0.80**	0.19	**0.03**
v02-Bistro	**0.74**	0.67	0.57	**0.77**	0.64	**0.72**	0.45	**0.15**
v03-Cambronne	**0.53**	0.51	0.60	**0.67**	0.56	**0.58**	0.88	**0.73**
v04-Navette	**0.70**	0.39	0.73	**0.74**	**0.71**	0.51	0.15	**0.05**
v05-Zara	0.70	**0.71**	0.60	**0.73**	0.63	**0.72**	0.55	**0.08**
Mean	**0.69**	0.62	0.61	**0.74**	0.63	**0.67**	0.44	**0.21**

Table 2: Comparison of performances and execution times between our tracker *TextTrail* and the tracker with detection (every 20 frames) *SnooperTrack*. Max recall, precision and *Fscores* per video in bold and minimum average computation times (in seconds) per frame in bold.

Figure 5: Example of application of our text tracker. First column presents a series of frames (33, 68, 96, 136) with embedded text. Second column gives binarized text area provided by a tracking and binarization process. Third column shows results of "inpainted" frames.

Mariani, R. (2002). A face location and recognition system based on tangent distance. In *Multimodal interface for human-machine communication*, pages 3–31. World Scientific Publishing Co., Inc.

Medeiros, H., Holgun, G., Shin, P. J., and Park, J. (2010). A parallel histogram-based particle filter for object tracking on simd-based smart cameras. *Computer Vision and Image Understanding*, (11):1264–1272.

Merino, C. and Mirmehdi, M. (2007). A framework towards real-time detection and tracking of text. In *CBDAR*, pages 10–17.

Minetto, R., Thome, N., Cord, M., Leite, N. J., and Stolfi, J. (2011). Snoopertrack: Text detection and tracking for outdoor videos. In *ICIP*, pages 505–508.

Phan, T. Q., Shivakumara, P., Lu, T., and Tan, C. L. (2013). Recognition of video text through temporal integration. In *ICDAR*, pages 589–593.

Schwenk, H. and Milgram, M. (1996). Constraint tangent distance for on-line character recognition. In *ICPR*, pages 515–519.

Simard, P., LeCun, Y., Denker, J., and Victorri, B. (1992). An efficient algorithm for learning invariances in adaptive classifiers. In *ICPR*, pages 651–655.

Tanaka, M. and Goto, H. (2008). Text-tracking wearable camera system for visually-impaired people. In *ICPR*, pages 1–4.

Tuong, N. X., Müller, T., and Knoll, A. (2011). Robust pedestrian detection and tracking from a moving vehicle. In *Proceedings of the SPIE*, volume 7878, pages 1–13.